Advances in Science and Technology Research Journal

Advances in Science and Technology Research Journal, 2026, 20(8), 130–145
https://doi.org/10.12913/22998624/220813
ISSN 2299-8624, License CC-BY 4.0

Received: 2026.02.27
Accepted: 2026.06.01
Published: 2026.07.01

Assessment of transient flow behavior and sensitivity analysis in the Al-Hashimiyah water treatment pipeline system using an integrated method of characteristics

Hayder Mohammed Kadhim[1], Mohammed S. Shamkhi[2,3], Ahmed Samir Naje[1*]

[1] Department of Water Resources Engineering Management, College of Engineering, Al-Qasim Green University, Babylon 51013, Iraq
[2] Department of Structures and Water Resources, Faculty of Engineering, University of Kufa, Najaf Al-Ashraf 54001, Iraq
[3] College of Engineering, University of Warith Al-Anbiyaa, Karbala 56001, Iraq
* Corresponding author's e-mail: ahmednamesamir@gmail.com

ABSTRACT

This study investigates transient flow behavior and the sensitivity of key hydraulic parameters in the Al-Hashimiyah water transmission pipeline under steady and unsteady flow conditions. Steady-state analysis yielded a flow velocity of 5.66 m/s, a Reynolds number of 1.18×10^6, and a Darcy-Weisbach friction factor of 0.008, with total head losses remaining below the allowable 70 m limit. A hybrid numerical model integrating the Method of Characteristics and Method of Integration (MOC–MOI) was developed and validated to simulate transient events, including sudden valve closures and pump shutdowns. Transient analysis indicated peak surge pressures of 205.13 m at a discharge of 0.34 m³/s, exceeding the safe operating range, while lower discharges (0.111 m³/s) limited surge pressures to 65.56 m. Pump failures induced severe pressure drops, with fluctuations reaching 95.9% of the initial head, generating negative pressures that risk cavitation. A surge tank (12 m diameter, 15 m height, 1.700 m³ volume) positioned 70 m downstream of the pumping station reduced peak pressures by 24.6%. Sensitivity analysis revealed that increasing pipe diameter from 0.24 m to 0.35 m reduced surge pressures from 191.21 m to 122.32 m, while higher friction (0.003–0.012) decreased surges from 187.40 m to 149.80 m. These findings confirm that the MOC–MOI model reliably predicts transient hydraulic behavior and provides an effective tool for design optimization, risk assessment, and operational planning in water transmission pipelines.

Keywords: transient flow, water hammer, surge tank, MOC-MOI hybrid model, pipeline system, sensitivity analysis.

INTRODUCTION

Pressurized water transmission systems are essential for delivering potable water to urban and rural communities. However, these systems are frequently exposed to transient hydraulic events caused by sudden operational changes such as rapid valve closure, pump shutdown, or unexpected power failure [1]. These disturbances generate pressure waves that propagate through the pipeline network, a phenomenon commonly referred to as water hammer. Such transient pressure fluctuations may exceed the allowable design limits of pipelines, potentially causing pipe rupture, structural damage, and operational failure of water supply systems [2, 3]. As water demand continues to increase due to population growth and urban expansion, understanding transient hydraulic behavior has become increasingly important for ensuring the safety and reliability of water infrastructure systems [4].

Numerous studies have investigated the factors influencing water hammer behavior in pressurized pipelines. Hydraulic parameters such as pipe diameter, pipe material elasticity, friction factor, and wave propagation velocity play a critical role in determining the magnitude and propagation of transient pressure waves [5, 6]. To analyze

these complex hydraulic phenomena, researchers have developed various analytical, numerical, and experimental approaches. Previous studies have examined the transient hydraulic response of pipeline systems and quantified the influence of several governing parameters. For instance, numerical simulations using the method of characteristics (MOC) have demonstrated that rapid valve closure can produce pressure surges exceeding 1.5 to 2.0 times the steady-state pressure head, depending on pipe length, wave speed, and boundary conditions [7, 8]. Similarly, investigations by Jalut and Ikheneifer [9] and Zhang et al. [10] showed that transient pressure heads in long-distance water transmission pipelines may increase by 80–120% above the initial operating pressure, particularly during pump trip or sudden valve closure events. These studies confirmed that the magnitude of pressure waves is strongly influenced by system geometry and operational conditions.

Several researchers have also evaluated the impact of pipeline material properties on transient pressure behavior. Kandil et al. [11] reported that pipelines constructed from materials with lower elastic modulus, such as polypropylene random (PPr) and unplasticized polyvinyl chloride (uPVC), can reduce peak surge pressures by approximately 15–30% compared with steel pipelines, due to their higher capacity for energy dissipation. In addition, Urbanowicz et al. [12] and Liu et al. [13] investigated pipeline strain and fatigue caused by transient pressure waves using combined numerical and analytical approaches. Their results indicated that the predicted strain response under water hammer loading could be simulated with an error of less than 7.56%, demonstrating the effectiveness of advanced numerical models in evaluating structural responses to transient loads.

Further developments in transient flow modeling have focused on improving the representation of hydraulic resistance during unsteady flow conditions. Mandair et al. [14] and Bruhl [15] proposed analytical formulations for frequency-dependent friction, showing that incorporating unsteady resistance terms significantly improves agreement between experimental measurements and numerical predictions, particularly for low water hammer numbers ($Wh \leq 0.1$). These results highlight the importance of accurately representing frictional effects when simulating transient flow behavior in pressurized pipelines.

Despite considerable progress in transient flow modeling, several aspects remain insufficiently explored in water transmission systems within developing regions. In particular, limited research in Middle Eastern infrastructure, including Iraq, has examined the combined effects of pipeline material elasticity, wave propagation characteristics, and valve operation dynamics on transient hydraulic behavior. Additionally, integrated numerical approaches for analyzing water hammer and system sensitivity under local operational conditions are still scarce, highlighting the need for comprehensive assessments to enhance the reliability and safety of regional water transmission networks.

To address these research gaps, the objective of this study is to evaluate transient flow behavior and conduct a sensitivity analysis of the Al-Hashimiyah water transmission pipeline system using an integrated numerical modeling framework. Specifically, this study aims to: (1) identify the key hydraulic parameters influencing transient flow behavior in the Al-Hashimiyah pipeline system; (2) develop and implement a coupled method of characteristics–method of integration (MOC-MOI) numerical model in MATLAB to simulate unsteady flow conditions; (3) perform a sensitivity analysis to investigate the effects of pipe diameter, discharge, and the Darcy–Weisbach friction factor on surge pressure characteristics; (4) evaluate mitigation strategies for reducing water hammer impacts, including optimized valve operation and surge protection devices; and (5) provide practical recommendations for improving the hydraulic performance, operational safety, and long-term efficiency of the water transmission system.

By integrating advanced numerical modeling with system-specific analysis tailored to local infrastructure conditions, this research provides improved understanding of water hammer behavior in Iraqi water supply systems and contributes to the development of more resilient and sustainable water transmission infrastructure.

MATERIALS AND METHOD

Case study description

The Al-Hashimiyah Water Treatment Plant, presented in Figure 1, located in the south of Babylon Governorate, Iraq, serves as the focus of the present study. It is a vital infrastructure project with a treatment capacity of 6.000 cubic meters per hour, providing potable water to over 250,000

residents across Al-Hashimiyah, Al-Qasim, Al-Tali'ah, Al-Shomali districts, and surrounding areas (Abulameer et al., 2024). The plant comprises six functional units: (1) low pumping unit, (2) sedimentation basins, (3) chemical processing unit, (4) filtration unit, (5) water storage unit, and (6) high pumping unit.

Raw water is drawn from the Al-Hilla/Al-Hashimiyah River through six iron pipelines (diameter: 0.25 m) into the low pumping unit (Figure 1 a and b). Water then flows through six circular sedimentation basins, each with a 1.000 m³ capacity, as shown in Figure 1 c, followed by treatment in the chemical unit where chlorine is added. Subsequently, it passes through the filtration unit, which consists of 32 filters arranged in four regions. The treated water is stored in tanks and finally distributed via ten pumps installed in the high pumping unit (Figure 1 d), each designated for specific districts.

Water transport path

Al-Hashimiyah is a key district located in the southern part of Babylon Governorate, Iraq, served by a major infrastructure facility.

The transport path of treated water within the plant starts at the filtration unit, where the filtered water is collected in specially designed storage tanks that are equipped with vent pipes to regulate air pressure and prevent vacuum conditions. From there, water is directed to the high pumping unit, which is the final stage in the treatment process. This unit consists of ten high-capacity pumps, each designated to supply water to the main service zones as follows:

- two pumps serve the Al-Hashimiyah district
- three pumps serve the Al-Qasim district
- three pumps supply the Al-Madhatiya district
- two pumps supply the Al-Shomali district

Each of the ten discharge pipes connected to these pumps has a diameter of 0.25 m and length of 500 m, and they play a critical role in conveying water under pressure to the main distribution network. As part of the current study, special attention is given to transient flow phenomena in these pipes, particularly the occurrence of water hammers. Water hammer, also known as hydraulic shock, is a potentially damaging surge of pressure resulting from the rapid deceleration or stoppage of flow such as sudden pump shutdown or valve closure. This phenomenon can pose serious risks to pipeline integrity and operational safety if not properly analyzed.

To address this, the study involves the simulation and evaluation of water hammer effects in the ten distribution pipes, all with a uniform diameter of 0.25 m, using numerical modeling techniques. A MATLAB-based computational model was developed to simulate the behavior of pressure waves and to predict the magnitude of pressure surges under different operating scenarios [16, 17]. Key parameters such as flow velocity, wave speed, and pipe material properties are

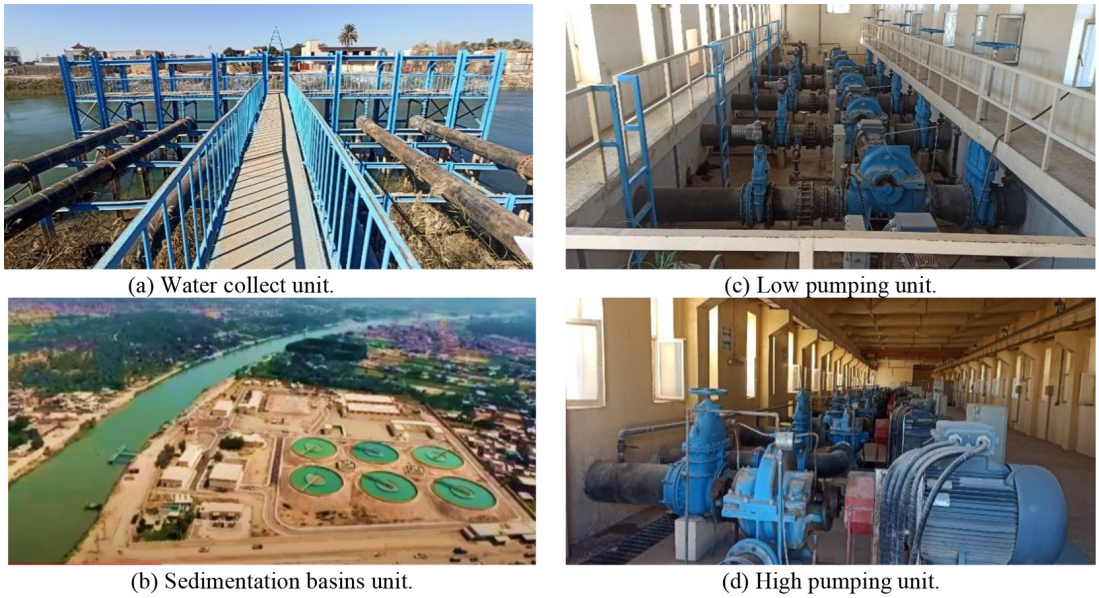

(a) Water collect unit. (c) Low pumping unit.

(b) Sedimentation basins unit. (d) High pumping unit.

Figure 1. Al-Hashimiyiah water treatment plant

incorporated into the model based on field data and design specifications from the Al-Hashimiyah plant.

The terrain through which the distribution pipelines extend is characterized as semi-flat and arable, allowing for stable pipe installation and minimal elevation-induced pressure variation [18, 19]. This analysis provides essential insights for improving system reliability, preventing failures, and designing effective surge protection measures for the Al-Hashimiyah water supply network.

Water demand calculations

The Al-Hashimiyah Water Treatment Plant is designed to meet water needs in the southern region of Babylon Governorate. It supplies treated water to the districts of Al-Hashimiyah, Al-Qasim, Al-Tali'ah, and Al-Shomali, serving an estimated population of 250,000 inhabitants in the base year 2025. To estimate future water demand, demographic data from the Statistics Division of Babylon Governorate was used. The population in the service area has shown a consistent upward trend. To forecast population growth from 2025 to 2050 for effective planning of water treatment capacity, pipeline design, and operational schedules, four demographic models were considered: Arithmetic (Linear), Geometric, Exponential, and Logistic. Given the area's relatively stable and predictable population growth, the Arithmetic (Linear) Model was selected [20–22]. This model assumes a constant increase in population each year and is expressed by the Equation 1:

$$r = \frac{P_t - P_0}{P_0} \quad (1)$$

where: r – population growth rate (%); P_0 – initial population at the base year; and P_t – projected population at year t.

Assuming a constant annual increase of 5.000 inhabitants, the projected population from 2025 to 2050 is illustrated in Figure 2.

Based on a per capita water consumption of 300 liters/day, as recommended by the Iraqi Ministry of Planning, the daily domestic water demand for the projected population in 2050 is calculated as follows:

$$375{,}000 \times 300 = 112{,}500{,}000 \text{ liters/day} = $$
$$= 1{,}30 \text{ m}^3 \text{/sec}$$

In addition to domestic use, water is also required for agriculture and public services. Thus, the total maximum discharge requirement is estimated at approximately 0.35 m³/sec. The existing design discharge capacity of the Al-Hashimiyah Water Treatment Plant is 6.000 m³/hr. (≈ 1.67 m³/sec). While this capacity adequately meets the current needs, it will require future upgrades to accommodate the growing population and expanded service requirements anticipated by 2050. This forecast provides a comprehensive basis for long-term infrastructure planning and water resource management for the Al-Hashimiyah service region.

Design parameters

As previously mentioned, the total length of the supply lines is approximately 500 meters from each of the four pumping stations to their respective service areas. The required discharge rates for

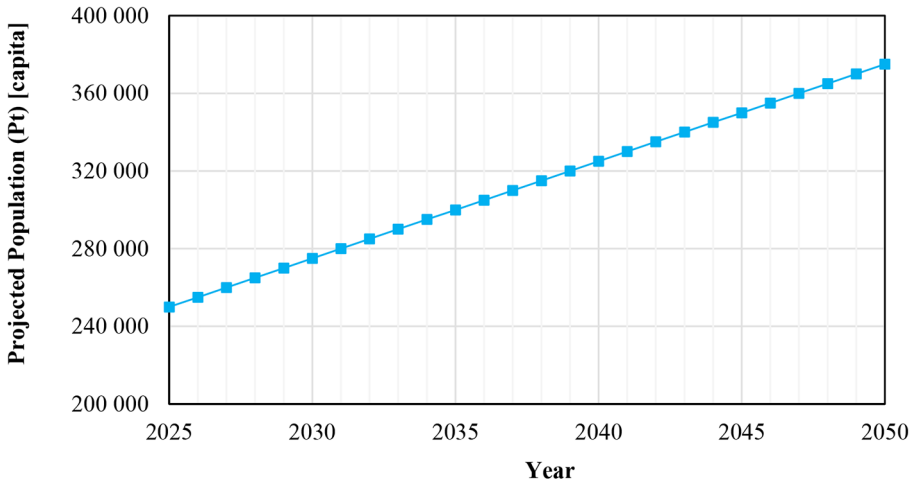

Figure 2. Projected population growth (2025–2050) using arithmetic model

each district are determined based on domestic water demands and are summarized in Table 1.

For each pump, the maximum current discharge required for the system is approximately 1000 m³/hr. (0.278 m³/s), based on current population estimates and domestic water demand. The pipeline system will use unplasticized polyvinyl chloride (PVC-U) pipes, in accordance with DIN 8062 (2009) standards. The pipes are circular with a diameter of 0.25 meters and a wall thickness of 0.01 meters. At 20 °C, the allowable working pressure heads for PVC-U pipes, assuming a 25-year design life and a safety factor of 2, is 7 bars (70 meters).

PROPOSED MODEL FORMULATION

General

The method of characteristics (MOC) is widely used for simulating water hammer due to its simplicity and suitability for long, prismatic pipelines, although explicit schemes may produce errors in short or variable-area sections [23–25]. Implicit methods offer unconditional stability and independence between space and time steps, making them preferable for short ducts, open channels, or non-prismatic geometries, albeit with higher computational effort [26]. Complex components such as draft tubes or surge tanks pose additional challenges, as simplified modeling may alter inertia distribution and affect accuracy [27–29]. To address these limitations, the present study adopts a hybrid MOC-MOI approach, employing MOC for long prismatic pipelines and MOI for short, variable-area, or free-surface sections, enhancing the precision and reliability of transient flow simulations.

Discretization of basic equations

The continuity and momentum equations governing transient flow in a variable-area duct are expressed as follows:

$$V\frac{\partial H}{\partial x}+\frac{\partial H}{\partial t}+\frac{a^2}{g}\frac{\partial V}{\partial x}+\frac{a^2 V}{gA}\frac{\partial A}{\partial x}-sin\beta.V=0 \quad (2)$$

$$g\frac{\partial H}{\partial x}+V\frac{\partial V}{\partial x}+\frac{\partial V}{\partial t}+\frac{f\,V\,|V|}{2D}=0 \quad (3)$$

where: x – distance; t – time; V – mean velocity; H – pressure head; a – wave speed; A – cross-sectional area; β v pipe slope; g – gravitational acceleration; f – Darcy-Weisbach friction factor; D – inner diameter of the pipe.

Both explicit (MOC) and implicit (Preissmann four-point finite difference) methods are applied to solve these water hammer equations.

The MOC transforms the quasi-linear hyperbolic PDEs into two groups of ODEs along characteristic lines, as shown in Figure (3, a) and as expressed. For a prismatic pipeline (i.e., $\partial A/\partial x = 0$), velocity is replaced by discharge, and the equations are integrated along the characteristic lines C^+ and C^-, yielding:

$$C^+: Q_p = C_p - B_p H_p \quad (4)$$

$$C^-: Q_p = C_M + B_M H_P \quad (5)$$

where:

$$B_p = \frac{1}{(C_0-C_2)/A+C_0C_1}$$

$$B_M = \frac{1}{(C_0+C_2)/A+C_0C_3}$$

$$C_p = B_p\left[Q_R\frac{C_0+C_2}{A}+H_R\right]$$

$$C_M = B_M\left[Q_S\frac{C_0-C_2}{A}+H_S\right]$$

$$C_0 = \frac{a}{g}$$

$$C_1 = \frac{f\Delta t|Q_R|}{2DA^2}$$

$$C_2 = \frac{1}{2}\Delta t\ sin\beta$$

$$C_3 = \frac{f\Delta t|Q_S|}{2DA^2}$$

Table 1. Summary of required discharges for each district

District	No. of pump	Q of pump 1 (m³/h)	Q of pump 2 (m³/h)	Q of pump 3 (m³/h)
Al-Hashimiyah	2	1000	1000	-
Al-Qasim	3	1000	1000	400
Al-Madhatiya	3	1000	1000	1000
Al-Shomali	2	700	700	-

Here, H_P and Q_P are the unknown pressure head and discharge at the future time $t + \Delta t$, while H_R and Q_R and H_S and Q_S are known values from the adjacent grid points at time t [30]. This implicit method uses a temporal weighting coefficient θ, and is unconditionally stable for $\theta \geq 0.5$. Second-order accuracy is achieved at $\theta = 0.5$. In this study, $\theta = 0.55$ is adopted.

Equation 6 represents the discretization of the Preissmann scheme corresponding to Figure 3, b.

$$f(x,t) = \frac{\theta}{2}(f_{i+1}^{n+1} + f_i^{n+1}) + \frac{1-\theta}{2}(f_{i+1}^{n} + f_i^{n})$$
$$\frac{\partial f}{\partial x} = \theta\frac{f_{i+1}^{n+1} + f_i^{n+1}}{\Delta x} + (1-\theta)\frac{f_{i+1}^{n} + f_i^{n}}{\Delta x} \quad (6)$$
$$\frac{\partial f}{\partial x} = \frac{f_{i+1}^{n+1} - f_i^{n+1} + f_{i+1}^{n} - f_i^{n}}{2\Delta t}$$

Applying the Preissmann scheme to Equations 2 and 3, the discrete control equatioare derived in incremental form:

$$A_1 \cdot \Delta H_{i+1} + B_1 \cdot \Delta Q_{i+1} = = C_1 \cdot \Delta H_i + D_1 \cdot \Delta Q_i + F_1 \quad (7)$$

$$A_2 \cdot \Delta H_{i+1} + B_2 \cdot \Delta Q_{i+1} = A_2 \cdot \Delta H_{i+1} + B_2 \cdot \Delta Q_{i+1} = \quad (8)$$

where:

$$A_1 = 1 + \theta\frac{\Delta t}{\Delta x}\left(\frac{Q_{i+1}}{A_{i+1}} + \frac{Q_i}{A_i}\right)$$

$$B_1 = \frac{a^2}{g\,A_{i+1}} \cdot \frac{2\theta\Delta t}{\Delta x}$$

$$C_1 = -1 + \theta\frac{\Delta t}{\Delta x}\left(\frac{Q_{i+1}}{A_{i+1}} + \frac{Q_i}{A_i}\right)$$

$$D_1 = \frac{a^2}{g\,A_i} \cdot \frac{2\theta\Delta t}{\Delta x}$$

$$F_1 = -\frac{\Delta t}{\Delta x}\left(\frac{Q_{i+1}}{A_{i+1}} + \frac{Q_i}{A_i}\right)(H_{i+1} - H_i) - \\ -\frac{a^2}{g}\frac{1}{2\Delta t}\frac{Q_{i+1}}{A_{i+1}} - \frac{Q_i}{A_i} - \frac{a^2}{g}\frac{\Delta t}{\Delta x}\left(\frac{Q_{i+1}}{A_{i+1}} + \frac{Q_i}{A_i^2}\right) \cdot \\ \cdot (A_{i+1} - A_i) + \Delta t\, sin\beta\left(\frac{Q_{i+1}}{A_{i+1}} + \frac{Q_i}{A_i}\right)$$

$$A_2 = g\theta\frac{\Delta t}{\Delta x}$$

$$B_2 = \frac{1}{2A_{i+1}}\left[1 + \theta\frac{\Delta t}{\Delta x}\left(\frac{Q_{i+1}}{A_{i+1}} + \frac{Q_i}{A_i}\right)\right]$$

$$C_2 = g\theta\frac{\Delta t}{\Delta x}$$

$$D_2 = \frac{1}{2A_i}\left[1 - \theta\frac{\Delta t}{\Delta x}\left(\frac{Q_{i+1}}{A_{i+1}} + \frac{Q_i}{A_i}\right)\right]$$

$$F_2 = -\frac{\Delta t}{2\Delta x}\left(\frac{Q_{i+1}^2}{A_{i+1}^2} + \frac{Q_i^2}{A_i^2}\right) - \\ - g\frac{\Delta t}{\Delta x}(H_{i+1} - H_i) - \\ -\frac{\Delta t}{2}\left(\frac{Q_i|Q_i|}{K_i^2} + \frac{Q_{i+1}|Q_{i+1}|}{K_{i+1}^2}\right)$$

$$K_i = A_i\sqrt{\frac{2D_i}{f}}$$

ΔH and ΔQ are the unknown increments in pressure head and discharge between time steps, and coefficients A1, B1, … F2 are calculated from previous time step values and known geometry. Since Equations 7 and 8 involve four unknowns per mesh node, the system remains open without

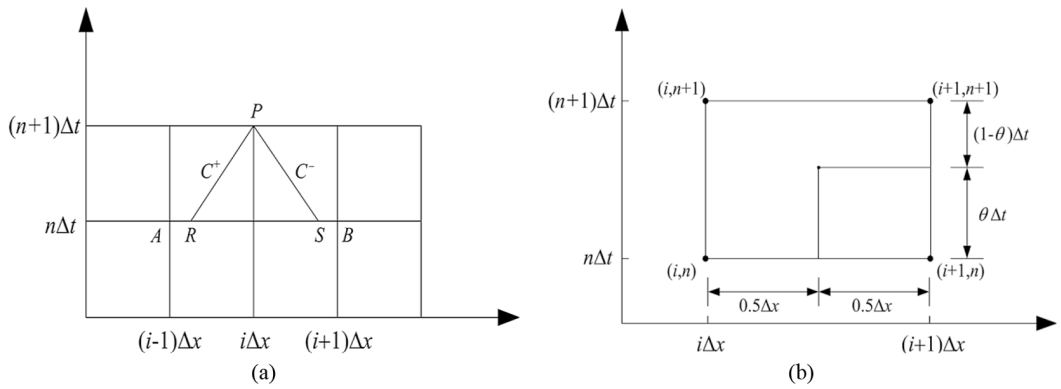

Figure 3. Method of characteristics and Preissmann scheme: (a) characteristic lines in the *x*–*t* plane using the MOC, (b) schematic diagram illustrating the Preissmann implicit finite difference method

boundary conditions. Therefore, two boundary conditions are necessary for the first and last nodes, forming a closed linear system of 2n equations with a bandwidth of 4 for n nodes [31].

Pipe and pump boundary conditions

To simulate the pump behavior during unsteady flow conditions, the following equations are employed:

Boundary equations for implicit pipes at the pump inlet and outlet:

$$Q_p = C_p - B_p \cdot H_p \tag{9}$$

$$Q_p = C_M + B_M \cdot H_s \tag{10}$$

where: Q_P is the pump discharge, H_P is the inlet pressure head, and H_S is the outlet pressure head.

Pump unit parameter equations:

$$Q_p = Q_1^0 D_1^2 \sqrt{(H_p - H_s) + \Delta H} \tag{11}$$

$$n_1^0 = \frac{nD_1}{\sqrt{(H_p - H_s) + \Delta H}} \tag{12}$$

$$M_t = M_1^0 D_1^3 (H_p - H_s + \Delta H) \tag{13}$$

where: Q_1^0, n_1^0, and M_1^0 represent the unit discharge, unit speed, and unit torque, respectively; D_1 is the pump diameter; and ΔH accounts for the velocity head difference between the spiral case outlet and draft tube inlet:

$$\Delta H = \left(\frac{\alpha P}{2g A_P^2} - \frac{\alpha S}{2g A_S^2} \right) Q_P^2 \tag{14}$$

where: αP, αS being the kinetic energy correction factors, and A_P, A_S the respective cross-sectional areas.

Pump characteristic curves:

$$Q_1^0 = f1(n_1^0, y) \tag{15}$$

$$M_1^0 = f2(n_1^0, y) \tag{16}$$

where: y denotes the guide vane opening.

Electric generator dynamics:

$$n = n^0 + \frac{0.1875 (M_t + M_t^0) \Delta t}{G D^2} \tag{17}$$

where: n is the rotational speed, GD^2 is the moment of inertia, and Δt is the time step.

Speed governor equation:

$$y = f(t) \tag{18}$$

This function defines the guide vane opening as a function of time during pump load rejection.

In the simulation, the flow direction does not influence the numerical solution due to the implicit nature of the pipe models. A forward scan is applied to IP1 (from upstream to downstream) to compute the characteristic equation C^+, while a backward scan is applied to IP2 (from downstream to upstream) to obtain C^-. The pressure head and discharge at each node are subsequently determined using the backward scanning method.

Larock et al. [32] showed that the wave's velocity equation can be traditionally written in the general form:

$$a = \frac{\sqrt{K/\rho}}{\sqrt{1 + \frac{KD}{E\,e}(C)}} \tag{19}$$

The equations are used to simulate the behavior of the pump under unsteady flow conditions. Where (K) is the bulk modulus of elasticity of the fluid, (ρ) is the bulk modulus of density of the fluid, (D) is the inner diameter of the pipe, (e) is the thickness of the pipe, (E) is the modulus of elasticity (Youngs modulus) of the pipe material and (C) is a coefficient that takes into account the pipe support conditions, C = 5/4−u, if pipe is anchored at the upstream end only [33].

- C = 1−u², if pipe is anchored against any axial movement.
- C = 1.0, if each pipe section is anchored with expansion joints at each section.

To accurately capture unsteady flow conditions within the surge tank system, a combination of the Method of Characteristics (MOC) and the Method of Integration (MOI) is adopted. The MOC is applied to the upstream and downstream pipelines, while the MOI is used to compute water level variations inside the surge tank.

Figure 4 illustrates the boundary node configuration. At node n, the free water surface elevation is known once the grid is generated.

The boundary conditions at node 1, which connects the surge tank to the pipelines, are governed by the following equations:

- Characteristic equations:

$$Q_s = C_P - B_p \cdot H_s \tag{20}$$

$$Q_x = C_M + B_M \cdot H_x \tag{21}$$

- Continuity equation:

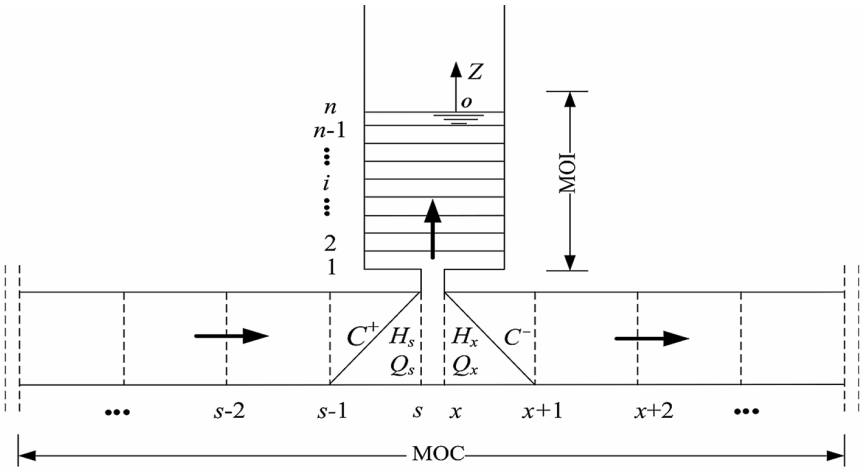

Figure 4. Coupling boundary conditions for surge tank

$$Q_s = Q_1 + Q_x \tag{22}$$

Energy equation:

$$H_s = H_x = H_1 + \alpha Q_1|Q_1| \tag{23}$$

where: Q_S, Q_x and Q_1 are the flow rates at different sections, H_S, H_x and H_1 are the corresponding heads, and α represents the energy loss coefficient associated with the surge tank entrance.

Combining Equations 20 to 23, the boundary equation at Node 1 is obtained in the incremental form:

$$\Delta Q_1 = EE_1 \cdot \Delta H_1 + FF_1 \tag{24}$$

An additional equation is used to enforce the boundary condition at Node *n*:

$$f(Q_n, H_n) = 0 \tag{25}$$

Currently, the key simulation parameters for the MOC-MOI model are explicitly defined to ensure accuracy and reproducibility. The pipeline was discretized into 100 nodes with a time step of 0.01 s. Initial conditions were based on steady-state flow, and boundary conditions included upstream/downstream pressure heads, valve dynamics, and surge tank levels. This setup reliably captures transient phenomena such as pressure surges and wave reflections.

RESULTS AND DISCUSSION

Model verification

To ensure the reliability of the proposed hybrid MOC-MOI model, a detailed verification procedure was conducted in MATLAB by comparing its predictions with published results from similar hydraulic systems. This approach allowed for quantitative evaluation of the model's accuracy, including analysis of errors and statistical performance metrics.

The first case was based on the study by Elbashir and Amoah [34], which modeled a hydraulic system consisting of two reservoirs with water surface elevations H_1 = 70 m and H_2 = 60 m, connected by a circular steel pipeline of length = 5.500 m, diameter = 0.4 m, and wall thickness 0.003 m. The pipeline friction factor was f = 0.009, and a butterfly valve upstream of the lower reservoir was used to control flow. Valve closure was simulated with Tc = 2L/a, where a = 950 m/s is the wave speed.

The MOC-MOI model accurately predicted transient pressure fluctuations, capturing both maximum and minimum pressures, the timing of wave reflections, and overall oscillation patterns. Quantitative comparison yielded a coefficient of determination (R^2) = 0.94 and a root mean square error (RMSE) = 3.8 m, indicating high agreement with the reference model and confirming the reliability of the predicted transient responses (Figure 5).

The second case followed Mansuri et al. [35], involving a pipeline of length = 4.800 m, diameter = 2 m, and static head of 100 m, with f = 0.022 and wave speed a = 1.200 m/s. Figure 6 shows the resulting transient pressure head predictions. The MOC-MOI model closely matched the reference results, particularly in reproducing peak surge pressures. Statistical assessment indicated R^2 = 0.92–0.96 and RMSE < 4.5 m, confirming both accuracy and consistency. To

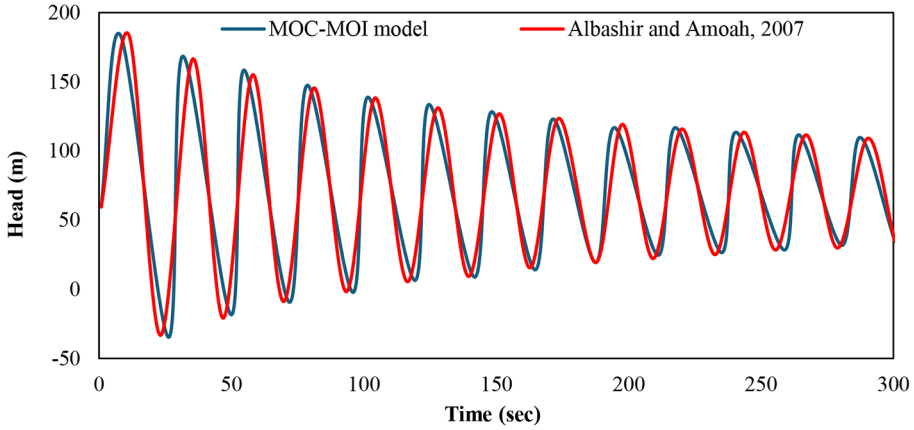

Figure 5. Comparison of transient pressure head response between the MOC-MOI model and Elbashir and Amoah [34] model

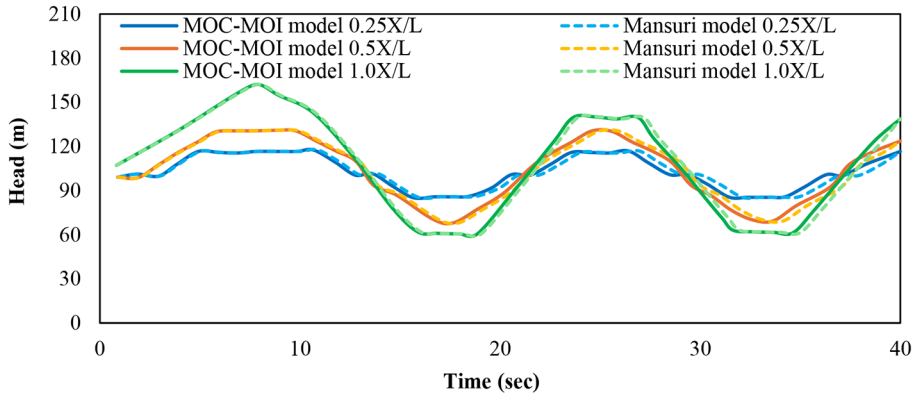

Figure 6. Comparison of transient pressure head between MOC-MOI model and Mansuri et al. [35] model

evaluate predictive reliability, the absolute and relative errors between the MOC-MOI model and reference data were calculated for maximum, minimum, and average pressure heads at multiple nodes. Maximum relative errors did not exceed 5.1%, and overall trends were accurately captured across all time steps, demonstrating robustness in both amplitude and timing predictions.

The verification confirms that the MOC-MOI model accurately simulates transient flow behavior, including surge pressures and wave reflections, supporting its reliable application for water hammer analysis and design optimization in real pipeline systems like Al-Hashimiyah.

Steady state calculations

Based on the topographic profile, the estimated water requirements and the pipe material considered, it was possible to estimate initial steady state conditions for head (H) and velocity (V). The flow velocity is derived from the continuity equation:

$$V = Q/A$$

where: Q = 0.278 m^3/s, A = $\pi D^2/4$ = π (0.25)^2/4 ≈ 0.0491 m^2 and V = 0.278/0.0491 ≈ 5.66 m/s.

The Reynolds number is calculated as: $Re + VD/v$ = 5.66 × 0.25/1.2 ×10 – 6 ≈1.18 · 10^6. Given a relative roughness of e/D = 0.01/0.25 = 0.0025, the Darcy-Weisbach friction factor, estimated from the Moody diagram, is approximately 0.008. The system includes:

Gate valves before pumping stations (loss coefficient K=0.17); Check valves after pumping stations (disk type, K=10)

Friction loss is calculated using the Darcy-Weisbach equation:

$$h_f = f \cdot \frac{L}{D} \cdot \frac{V^2}{2g} = 0.008 \cdot \frac{500}{0.25} \cdot \frac{5.66^2}{2 \cdot 9.81} \approx 5.24 \text{ m}$$

The addition of head requirements per segment, including losses and friction, is checked to be less than the allowable 70 meters pressure

head. Using these four values, the system needs four working input pumping stations located along 500-m stretches to provide adequate pressure and flow to operate efficiently.

Transient flow calculations

In hydraulic transient, the behavior of water hammer and pressure fluctuations on the length of pipeline would be assessed. To calculate the hydraulic transient due to valve closure, MATLAB software language has been written. The hybrid MOC-MOI is used to solve the governing equations. The wave's velocity (a), could be determined by equation (19) where the bulk modulus of elasticity of water $K = 2.15 \times 10^9$ Pa, and the density of water $\rho = 1000\ kg/m^3$, Young modulus (modulus of elasticity) for iron $E = 200 \times 10^9$ Pa, Poisson ratio for iron $\mu = 0.3$, diameter of the pipe $D = 0.25\ m$, and the thickness of the pipe wall $e = 0.01$ m. Use the $C = 1-\mu^2 = 0.91$ (pipe is anchored against any axial movement) because it gives us maximum value of wave's velocity.

$$a = \frac{\sqrt{2.15\times10^9/1000}}{\sqrt{1+\frac{2.15\times10^9\times0.25}{200\times10^9\times0.01}}} = 1314.4 \text{ m/s}$$

The upstream and downstream boundary conditions are used to get values of (HP) and (VP) at each end of the pipe. The whole process begins again using the just computed values of (HP) and (VP) as the known values. The process continues to loop until the time has reached the end of time. Before execution is terminated, values of (H) are printed for each node.

For simulation purposes, a valve closure time of 60 s was adopted. This value is greater than the pipeline's characteristic time $t_c = 2L/a \approx 10.5$ s, representing a moderately rapid closure scenario that can realistically occur during plant operations while producing measurable but safe surge pressures. The computed pressure fluctuations are shown in Figure (7a to d).

Hydraulic transient due to pump power failure

Rapid pump shutdowns can induce severe transient effects in the pipeline, potentially causing the hydraulic head at the pumping station to drop below the vapor pressure, leading to vapor column separation. Simulation results (Figure 8a–d) indicate that pressure fluctuations are significant, with

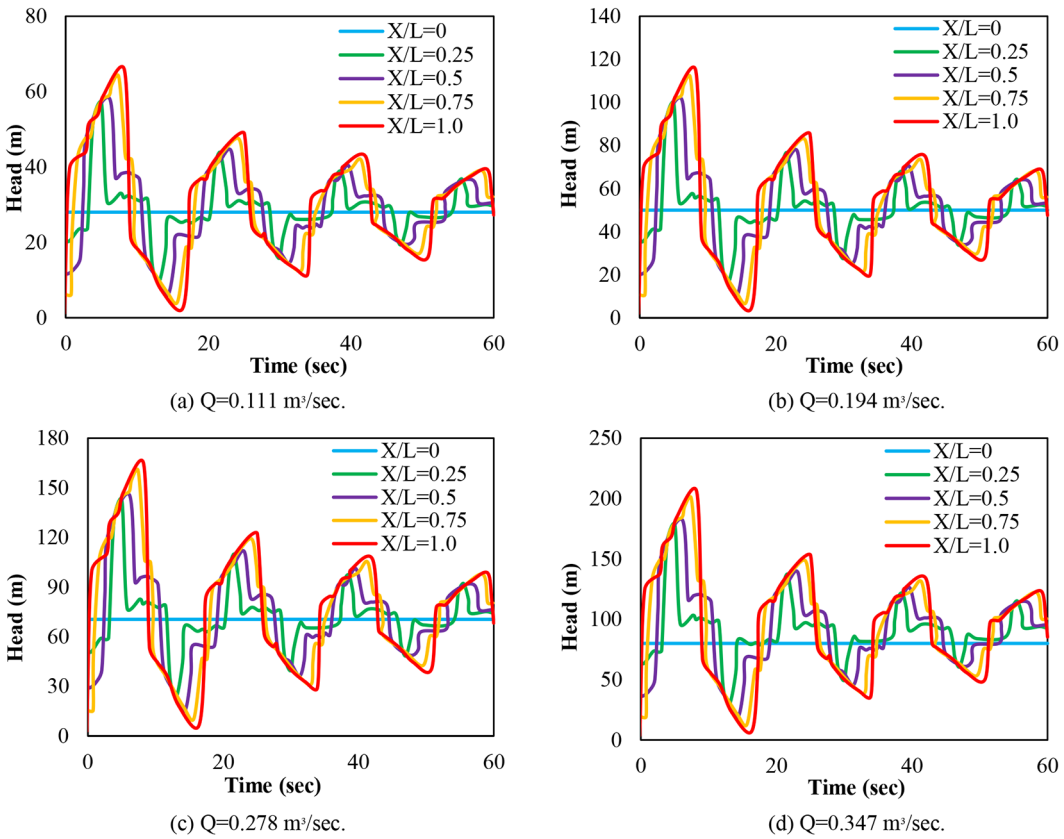

(a) Q=0.111 m³/sec. (b) Q=0.194 m³/sec.

(c) Q=0.278 m³/sec. (d) Q=0.347 m³/sec.

Figure 7. Pressure fluctuations at different positions of pipe (unprotected) (D=0.25m, f=0.008

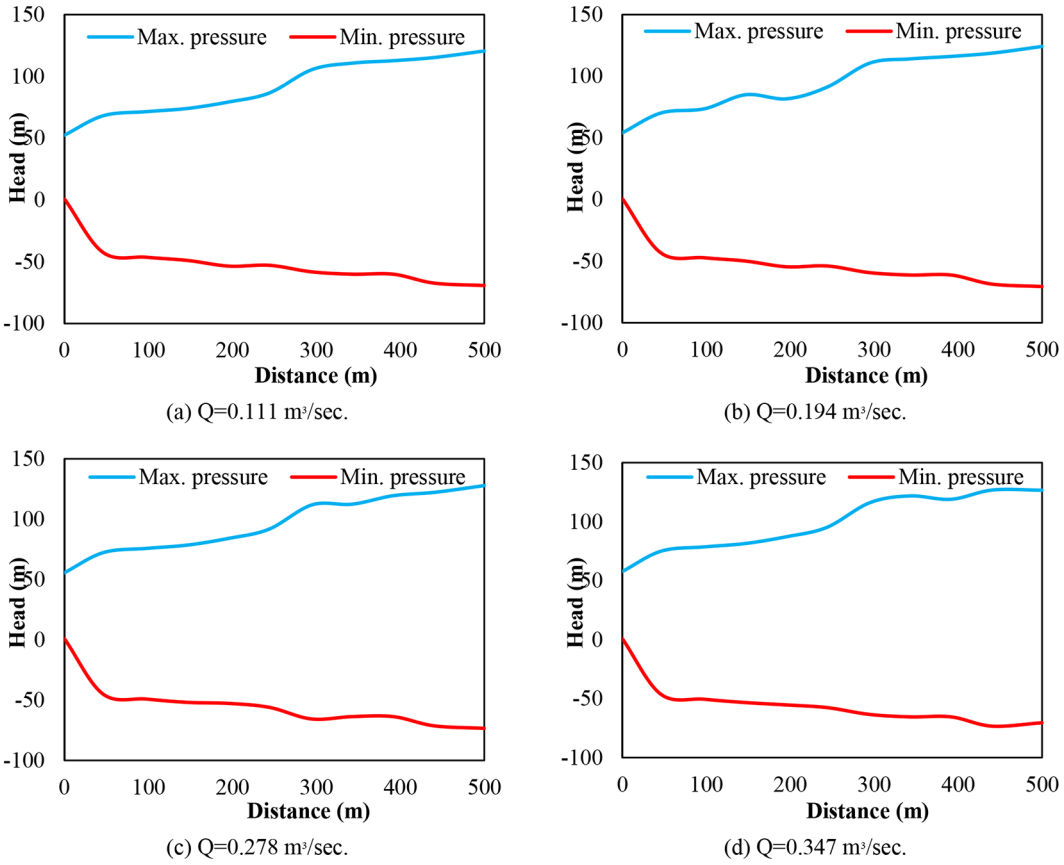

(a) Q=0.111 m³/sec. (b) Q=0.194 m³/sec.

(c) Q=0.278 m³/sec. (d) Q=0.347 m³/sec.

Figure 8. Maximum and minimum pressure along pipeline at pump stopping (D=0.25 m, f=0.008)

peak pressures increasing by approximately 95.7% during the first stage, 95.9% in the second stage, and 80.7% in the third stage relative to the initial pressure head. These findings highlight the critical importance of accurately modeling pump-induced transients to predict column separation and associated pressure surges in the pipeline system.

Mitigation for water hammer in case of valve closure

To protect the Al-Hashimiyah Water Treatment Plant pipeline system and mitigate the adverse effects of water hammer from sudden valve closures or pump stoppages, a surge tank is recommended. Water hammer generates transient pressure fluctuations that can cause pipe rupture, joint failure, or equipment damage. A surge tank stabilizes the system by absorbing or supplying water during these events, maintaining safe pressure levels.

The proposed surge tank is an open cylindrical structure hydraulically connected to the pipeline, with its normal water level aligned to the steady-state hydraulic grade line. During pump shutdowns, it supplies water by gravity, while during valve closure, it absorbs excess flow, reducing pressure spikes. For a flow rate of 0.347 m³/s, the tank is designed with a 12 m diameter (cross-sectional area ≈113 m²) and a 15 m height, providing ~1.700 m³ of storage. It is located 70 m downstream of the first pumping station. Transient simulations show that this configuration effectively controls both high-pressure surges and low-pressure vacuum events, ensuring that pressures remain within safe operational limits and prevent cavitation. Figure 9 illustrates the tank's layout and impact on the system, while Figure 10 shows that peak pressure at the pipe end is reduced by 24.6% compared to the unmitigated pipeline. This demonstrates that the surge tank is a vital solution to enhance the resilience and operational safety of the Al-Hashimiyah water network.

SENSITIVITY ANALYSIS

This section includes sensitivity analysis of flow properties of water hammer on a system including a pipe with variable diameter, discharge and friction factor would be assessed.

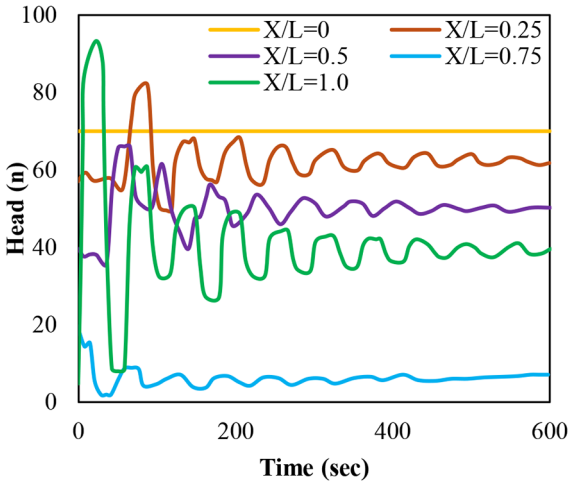

Figure 9. Pressure fluctuations at different positions of pipe (unprotected) (D=0.25 m, f=0.008, Q=0.347 m³/s)

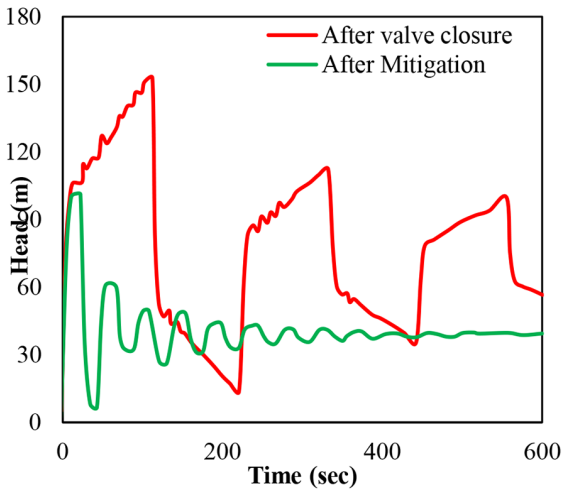

Figure 10. Comparison between protected and unprotected systems (D=0.25 m, f=0.008, Q=0.347 m³/s)

Sensitivity analysis for different pipe diameters

The sensitivity analysis on pipe diameter reveals a clear inverse relationship between pipe size, flow velocity, and maximum surge pressure under sudden valve closure conditions. Using a constant flow rate of 0.278 m³/s, friction factor of 0.008, wave velocity of 1314.4 m/s, and initial pressure head of 50 m, four pipe diameters were evaluated: 0.20 m, 0.25 m, 0.30 m, and 0.35 m.

Results indicate that smaller diameters produce higher velocities and surge pressures, with the 0.20 m pipe reaching 8.85 m/s and a maximum surge of 191.21 m. The baseline 0.25 m diameter reduced velocity and surge to 5.66 m/s and 164.15 m, respectively. Larger diameters further mitigated transient effects: 0.30 m resulted in 3.93 m/s and 139.37 m, while 0.35 m produced the lowest velocity (2.89 m/s) and surge pressure (122.32 m). These findings demonstrate that increasing pipe diameter effectively reduces pressure surges, mitigates hydraulic shock, and enhances the overall stability and safety of the water transmission system (Figure 11).

Sensitivity analysis for different discharge values

The sensitivity analysis on discharge demonstrates a direct relationship between flow rate, velocity, and maximum surge pressure under sudden valve closure conditions. With a fixed pipe diameter of 0.25 m, wave velocity of 1314.4 m/s, friction factor of 0.008, and initial pressure head of 50 m, four discharge scenarios were evaluated: 0.111, 0.194, 0.278, and 0.347 m³/s.

Results indicate that lower discharges produce modest surge pressures (65.56 m at 0.111 m³/s), while higher discharges generate more severe transients (205.13 m at 0.347 m³/s). Intermediate flows yielded proportionate surge pressures of 114.55 m (0.194 m³/s) and 164.15 m (0.278 m³/s).

These findings highlight that elevated flow rates significantly increase the risk of damaging pressure surges, emphasizing the need for appropriately sized surge protection and operational strategies in high-flow conditions to ensure pipeline safety and reliability (Figure 12).

Sensitivity analysis for different friction factors

The third sensitivity analysis highlights the impact of the Darcy-Weisbach friction factor on transient surge pressures. With a fixed discharge of 0.278 m³/s, pipe diameter of 0.25 m, wave velocity of 1314.4 m/s, and initial pressure head of 50 m, four friction factors were evaluated: f = 0.003, 0.006, 0.008 (baseline), and 0.012.

Results demonstrate a clear damping effect of friction on surge pressures. The lowest friction factor (f = 0.003) produced the highest surge pressure of 187.40 m, while increasing the factor to 0.006, 0.008, and 0.012 reduced the peak pressures to 175.20 m, 164.15 m, and 149.80 m, respectively. These findings emphasize that smoother pipes, though efficient under steady

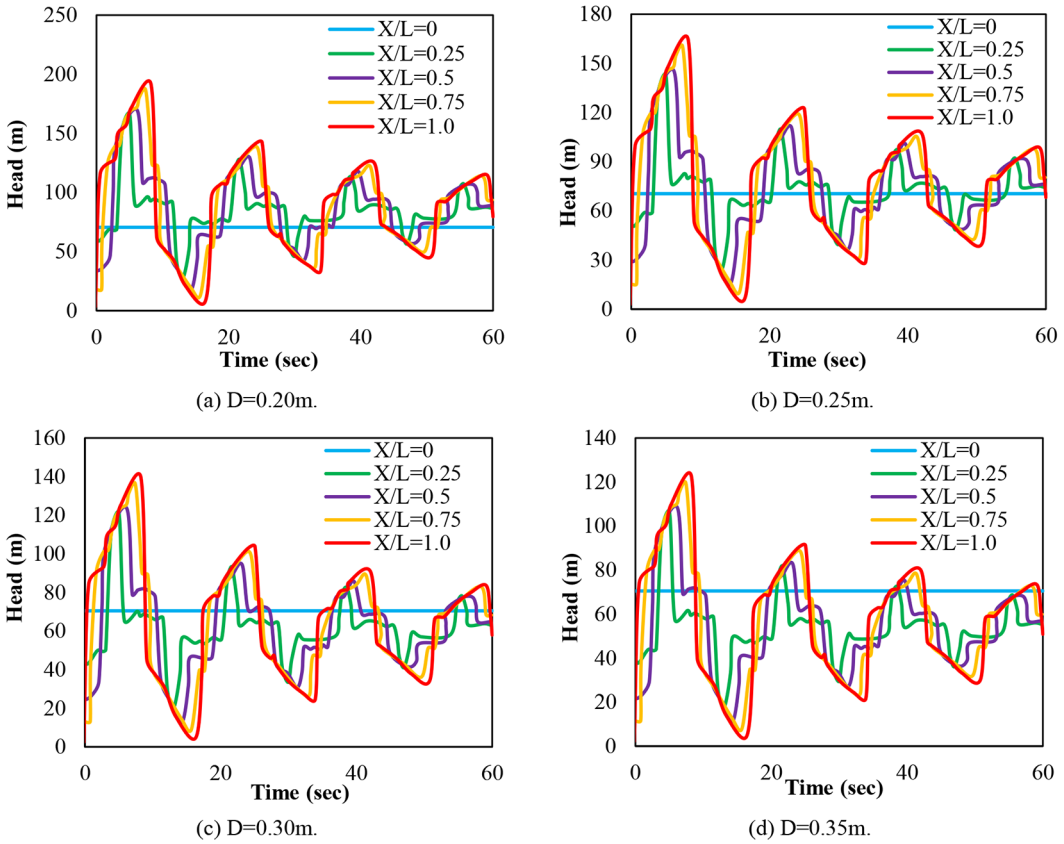

(a) D=0.20m. (b) D=0.25m.

(c) D=0.30m. (d) D=0.35m.

Figure 11. Surge pressure fluctuations at different positions of pipe (unprotected) under f=0.008 and a=1314.4 m/s

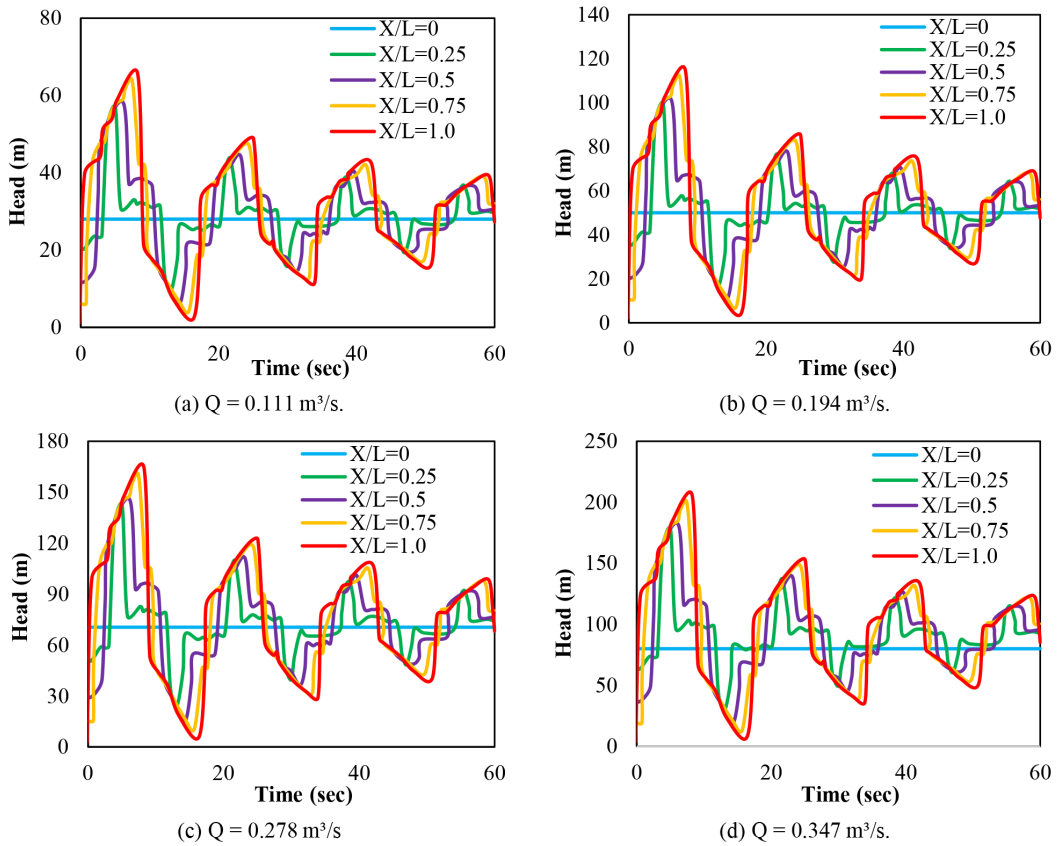

(a) Q = 0.111 m³/s. (b) Q = 0.194 m³/s.

(c) Q = 0.278 m³/s (d) Q = 0.347 m³/s.

Figure 12. Surge pressure fluctuations at different positions along the pipe (unprotected) under D = 0.25 m

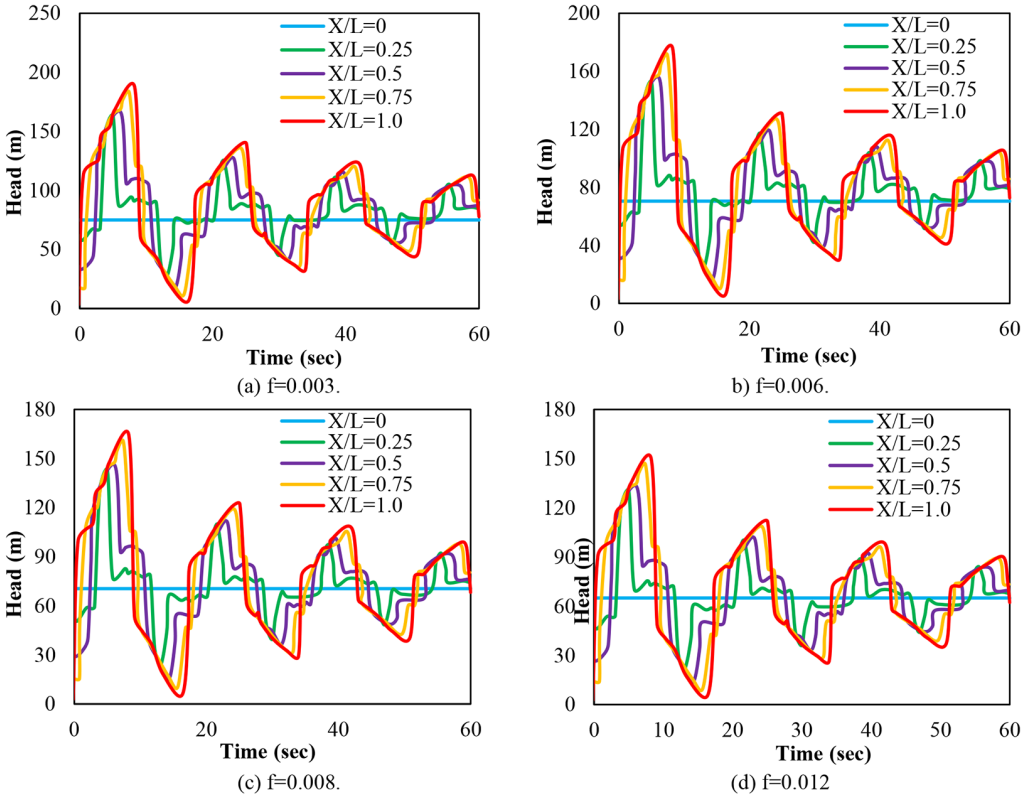

Figure 13. Surge pressure fluctuations at different positions along the pipe (unprotected)

flow, are more susceptible to elevated surge pressures, whereas rougher or aged pipes provide intrinsic damping, mitigating water hammer effects. Accurate estimation of the friction factor is therefore critical for transient pressure prediction and the design of effective surge protection measures (Figure 13).

CONCLUSIONS

Based on a detailed investigation of steady and unsteady flow conditions in the Al-Hashimiyah water transmission system, the following key findings were derived:

1. Steady-state analysis yielded a velocity of 5.66 m/s, a Reynolds number of 1.18×10^6, and a Darcy-Weisbach friction factor of 0.008, with total head losses remaining below the 70 m design limit.
2. The hybrid MOC-MOI model accurately simulated transient flow behavior, confirming its reliability for hydraulic assessments and water hammer analysis.
3. Rapid valve closures caused significant pressure surges, particularly at downstream sections, reaching near-critical thresholds under high discharge rates (up to 0.347 m^3/s).
4. Sudden pump stoppages led to extreme pressure drops and negative pressures, increasing the risk of cavitation and column separation.
5. The installation of a surge tank (12 m diameter, 15 m height, ~1.700 m^3 volume) located 70 m downstream from the first station effectively reduced peak pressures by 24.6%.
6. Sensitivity analysis showed that increasing pipe diameter from 0.20 m to 0.35 m reduced surge pressure from 191.21 m to 122.32 m, while higher friction factors (from 0.003 to 0.012) decreased peak surge from 187.40 m to 149.80 m. Surge pressures rose nonlinearly with increasing flow rate, from 65.56 m at 0.111 m^3/s to 205.13 m at 0.347 m^3/s.

The results show that the MOC-MOI hybrid method effectively captures key pressure transient dynamics, offering a flexible and reliable tool for pipeline design, operational planning, and risk assessment. Future work should incorporate field data, advanced pipe material behavior, multi-component networks, and optimized surge mitigation while considering climate and demand changes to further enhance the accuracy, resilience, and efficiency of water transmission systems such as Al-Hashimiyah.

Acknowledgments

The authors thank Al-Qasim Green University and the University of Kufa for their support in conducting this research.

REFERENCES

1. Zhao, L., Yang, Y., Wang, T., Han, W., Wu, R., Wang, P., Zhou, L. An experimental study on the water hammer with cavity collapse under multiple interruptions. Water, 2020; 12(9): 2566.
2. Pal, S., Hanmaiahgari, P. R., Karney, B. W. An overview of the numerical approaches to water hammer modelling: The ongoing quest for practical and accurate numerical approaches. Water, 2021; 13(11): 1597.
3. Wang, Y., Wang, T., Ran, Y., Zhang, X., Guo, X., Liu, S. The water hammer characteristics of long-distance water pipelines under different water supply modes. Water, 2024; 16(14): 2008.
4. Jalut, Q. H., Rasheed, N. J. Mathematical modeling for water hammer in pipe flow. Journal of Engineering and Sustainable Development, 2018; 22(1): 95–108.
5. Mansuri, B., Salmasi, F., Bakhshayesh, B. O. Sensitivity analysis for water hammer problem in pipelines. Iranica Journal of Energy and Environment, 2014; 5(2): 124–131.
6. Luan, W., Li, X., Kuang, W., Su, J., Xue, H., Zhang, K., Li, G. Quantitative assessment of the water stress in the Tigris–Euphrates river basin driven by anthropogenic impacts. Remote Sensing, 2025; 17(4).
7. Burgos, Ó. J., Coronado-Hernández, O. E., Ramos, H. M., Arrieta-Pastrana, A., Pérez-Sánchez, M. Water hammer mitigation using hydro-pneumatic tanks: A multi-criteria evaluation of simulation tools and machine learning modelling. Water, 2025; 17(13): 1883.
8. Wang & Yang. MOC-MOI hybrid method for better stability in hydraulic systems. 2015.
9. Jalut, Q. H., Ikheneifer, A. A. Mathematical simulation for transient flow in pipe under potential water hammer. Diyala Journal of Engineering Science, 2010; 22(23): 222–236.
10. Zhang, B., Wan, W., Shi, M. Experimental and numerical simulation of water hammer in gravitational pipe flow with continuous air entrainment. Water, 2018; 10(7): 928.
11. Kandil, M., El-Sayed, T. A., Kamal, A. M. Unveiling the impact of pipe materials on water hammer in pressure pipelines: an experimental and numerical study. Scientific Reports, 2024; 14(1): 30599.
12. Urbanowicz, K., Bergant, A., Karadžić, U., Jing, H., Kodura, A. Numerical investigation of the cavitating flow for constant water hammer number. Journal of Physics: Conference Series, 2021; 1736(1): 012040.
13. Liu, H., Li, J., Hua, T. F., Qiu, Y. Y. Research on the simulation method of dynamic characteristics of hydraulic pipelines under water hammer impact. Strength, Fracture and Complexity, 2025; 15672069241310694.
14. Mandair, S., Magnan, R., Morissette, J. F., Karney, B. Energy-based evaluation of 1D unsteady friction models for classic laminar water hammer with comparison to CFD. Journal of Hydraulic Engineering, 2020; 146(3): 04019072.
15. Bruhl, M. Analytical solution for laminar water hammer with frequency-dependent friction. Journal of Fluids Engineering, 2022; 144(11): 111302.
16. Nault, J. D., Karney, B. W. Improved rigid water column formulation for simulating slow transients and controlled operations. Journal of Hydraulic Engineering, 2016; 142(9): 04016025.
17. Swatridge, L. L., Mulligan, R. P., Boegman, L., Shan, S. Development and performance of a high-resolution surface wave and storm surge forecast model: application to a large lake. Geoscientific Model Development, 2024; 17(21): 7751–7766.
18. Leary, D., Theriault, B., Sommerville, A., Nixon, M. The importance of terrain analysis for pipeline planning and pipeline asset management. In Pipelines 2018 (pp. 245–255). Reston, VA: American Society of Civil Engineers.
19. Shehab, E. Q., Alsultany, R. A new approach to sustainable environmental assessment for wastewater treatment plants-A case study in the central region of Iraq. Ecological Engineering & Environmental Technology (EEET), 2025; 26(1). https://doi.org/10.12912/27197050/194126
20. Scholten, L., Maurer, M., Lienert, J. Comparing multi-criteria decision analysis and integrated assessment to support long-term water supply planning. PloS one, 2017; 12(5), e0176663.
21. Saber, Q.A., Riyadh, A., Al-Saadi, A.A., Karim, I.R., Khassaf, S.I., Mohammed, O.I., Abed, S.M., Naser, R.A., Hussein, A., Muslim, F., Naimi, S., Salahaldain, Z. Structural finite element analysis of bridge piers with consideration of hydrodynamic forces and earthquake effects for a sustainable approach. Mathematical Modelling of Engineering Problems, 2025; 12(3): 1071–1080. https://doi.org/10.18280/mmep.120334
22. Alsultani, R., Hasan, R. F. Novel mathematical model for long-term hydrodynamic evolution of sediment transport and its impact on meandering geometry. Journal of Water and Land Development, 2026; 1–16.
23. Mao, X., Wen, G., Wang, Y., Hu, J., Gan, X., Zhong, P. Development of WHED method to study operational stability of typical transitions in a hydropower plant and a pumped storage plant. Energies, 2025; 18(6): 1549.
24. Moradi, J., Andwari, A. M., Könnö, J. Numerical methods for the flow fields; A comparative review.

Scandinavian Simulation Society, 2025; 472–480.

25. Tukenova, L., Auyelbekov, O., Sapakova, S., Abduraimova, B., Ualiyev, Z., Kabdoldina, A.,... Kalpebaev, A. R. Research of the finite difference numerical method using artificial intelligence for solving problems of incompressible fluid flow in a rectangular domain with initial and boundary conditions. Engineered Science, 2025; 34: 1416.
26. Wang, W., Wu, Y., Wu, H., Yang, C., Feng, Q. Numerical analysis of dynamic compaction using FEM-SPH coupling method. Soil Dynamics and Earthquake Engineering, 2021; 140: 106420.
27. Assaf, M. Modeling and understanding flow transients in unusual cases in water systems (Doctoral dissertation, Politecnico di Torino). 2024.
28. Goncalves, R. A geometrically exact beam finite element for non-prismatic strip beams: The spatial case. International Journal of Structural Stability and Dynamics, 2024; 24(12): 2450138.
29. Alsultani, R., Abdulwahd, A. K., Hasan, A. R., Afan, H. A. A tiered hybrid life cycle assessment for sustainable water resources management in Iraq. Civil and Environmental Engineering, 2025; 22(2), Sciendo, https://doi.org/10.2478/cee-2025-0098
30. Sagar, H. J., et al., Moctar, O. Numerical simulation of a laser-induced cavitation bubble near a solid boundary considering phase change. Ship Technology Research, 2018; 65(3): 163–179.
31. He, J., Hou, Q., Yang, X., Duan, H., Lin, L. Isolated slug traveling in a voided line and impacting at an end orifice. Physics of Fluids, 2024; 36(2).
32. Larock, B. E., Jeppson, R. W., Watters, G. Z. Hydraulics of pipeline systems. CRC Press. 1999.
33. Alsltani, R., Rwayyih Hasan, A., Talib Al-Yasir, A. Joint hazard fragility analysis of pile foundation bridge piers in coastal soft soil areas subjected to water waves and earthquake actions. ISH Journal of Hydraulic Engineering, 2025; 31(5): 1017–1043. https://doi.org/10.1080/09715010.2025.2564792
34. Elbashir, M., Amoah, S. Hydraulic Transient in a Pipeline (Using Computer Model to Calculate and Simulate Transient), M.Sc. Thesis, Department of Building and Environmental Technology; Lund University. 2007.
35. Mansuri, B., Salmasi, F., Bakhshayesh, B. O. Sensitivity analysis for water hammer problem in pipelines. Iranica Journal of Energy and Environment, 2014; 5(2): 124–131.